

# PVA-based electrospun nanofiber mats of potential use in active packaging

M. Félix<sup>1</sup>, C. Jiménez<sup>2</sup>, A. Romero<sup>3</sup>, A. Guerrero<sup>4\*</sup>

Department of Chemical Engineering, University of Sevilla, 41012 Sevilla, Spain

\* Corresponding author. Tel.: +34 954 557179 Fax +34 954 556441

E-mail address: aguerrero@us.es (M. Félix).

**Abstract**— *The aim of this study has been devoted to the study of electrospun polymeric nanofiber mats that can be potentially used in active packaging. A previous characterization of the PVA solutions was carried out. Thus, density, electrical conductivity and viscosity have been measured as a function of PVA concentration (0, 4, 7 and 10% w/w). Subsequently, a standard electrospinning process was carried out. The fiber diameter was determined by analyzing high-resolution images from Scanning Electron Microscopy (SEM) using Image J software. Moreover, a characterization of tensile properties (by means of DMA) and vapour sorption capacity of PVA-based nanofiber mats was performed. In addition, water-soluble compounds were incorporated into electrospun nanofiber mats. Although they may induce marked changes in morphology, their incorporation may lead to marked improvements in techno-functional properties. Thus, addition of Sodium Carbonate (SC) involves occurrence of beads, due to the increase in electrostatic charges, whereas Citric Acid (CA) induce an increase in fiber size, related to a loss of solvent evaporation efficiency. However, both compounds significantly enhance water vapour absorption capacity.*

**Keywords**— *Electrospinning, DMA, Nanofibers, Active Packaging, PVA.*

## I. INTRODUCTION

The use of proper packaging materials and methods to minimize food deterioration, while providing safe and wholesome food products has always been the focus of food packaging. Current trends in consumer preferences have stimulated research into novel packaging concepts that actively play a role in the preservation of foods, through either absorption or release of compounds, known as active packaging (Siripatrawan & Vitchayakitti, 2016). Active packaging technologies interact with the internal gas environment in order to improve the food preservation or sensory properties while maintaining the quality and safety of the packaged food. Such newly employed technologies use substances to continuously modify the gas environment (and may interact with the product surface) by removing or adding gases in the headspace inside the package (Janjarasskul, Tananuwoong, Kongpensook, Tantratian, & Kokpol, 2016).

The internal atmosphere may be controlled by substances that absorb (scavenge) or release (emit). Polymers, due to their inherent ability to allow the passage of low molecular weight compounds, are the materials of choice for these novel packaging concepts. Some examples of active-packaging systems are O<sub>2</sub> scavengers, CO<sub>2</sub> emitters, ethylene absorbers, moisture regulators, taint removal systems, ethanol emitters and antimicrobial-releasing systems (Bodbodak & Rafiee, 2016; Lucera, Conte, & Nobile, 2016; Siripatrawan & Vitchayakitti, 2016). O<sub>2</sub> scavengers or CO<sub>2</sub> emitters frequently associated with Modified Atmosphere Packaging (MAP) systems, can be incorporated into polymer packaging by addition to the master batch via solution or dispersion, or they can be included in an inner layer in the case of multi-layer materials (Sandhya, 2010). Designing materials with scavengers or emitters requires the active polymer to be capable of being processed into packaging materials by conventional methods, while maintaining its properties as a container after the active agent has been exhausted. For meat preservation, CO<sub>2</sub> emitters are commonly used because of their inhibitory activity against a range of aerobic bacteria and fungi, being the only one displaying a direct antimicrobial effect, among the most frequently used gases in MAP systems. In fact, O<sub>2</sub> scavengers/CO<sub>2</sub> emitters are becoming increasingly attractive to food manufacturers and retailers and the growth outlook for the global market is bullish (Arvanitoyannis & Oikonomou, 2012).

The fibres material, specifically electrospun fiber mat with submicron fiber diameters (100-300 nm) and exceptionally high surface area could readily overcome this problem. The electrospinning process has proven to be a facile approach for the fabrication of 3D fiber mats and recently functional nanofibers have been proposed, specifically through the immobilization/encapsulation of food ingredients or enzymes/proteins within the electrospun matrix (Fernandez, Torres-Giner, & Lagaron, 2009; Tang, Liu, Hou, & You, 2011). The 3D structure of electrospun fiber mat acts as a passive barrier in food packaging and it can also exhibit higher antimicrobial activity. Therefore, electrospun fibres with incorporated

enzymes (as antimicrobial agent) could be ideal as food packaging materials where they can act as killing agent and/or inhibit bacteria growth on surface of foods and allow or facilitate the development of new and healthier food products.

Additionally, fiber diameter and fiber mat architectures are tuneable by simply varying process and material parameters such as cospinning polymer, solution viscosity and conductivity, voltage, flow rate, nozzle-collector distance, and collection method (Bhardwaj & Kundu, 2010). Electrospun nanofibers offer many advantages over traditional fibres including high surface area to volume ratio, tuneable porosity, and ease of manipulating fiber chemical compositions and structures for desired properties and functionalities. While electrospinning serves as a technique with great potential for the delivery of ingredients for functional food products and active packaging, several challenges remain unresolved (Bhushani & Anandharamakrishnan, 2014).

The aim of this work has been to study new materials of potential use in active packaging. To achieve this objective, new electrospun mats, which exhibit novel properties related to food preservation such as CO<sub>2</sub> release, have been evaluated. Polyvinyl alcohol (PVA) aqueous solutions have been processed through electrospinning at different PVA concentrations. Electrospun PVA nanofiber mats have been characterized by means of Dynamic Mechanical Analysis (DMA), using both oscillatory dynamic and uniaxial tensile tests, and Scanning Electron microscopy (SEM). In addition, water vapour absorption capacity was determined. To improve this ability, the effect of addition of two different compounds was also evaluated: Sodium Carbonate (SC) and/or Citric Acid (CA)...

## II. MATERIALS AND METHODS

### 2.1 Materials

Polyvinyl alcohol (PVA), Sodium Carbonate (SC) and Citric Acid (CA) were purchased from Sigma & Aldrich (Zwijndrecht, The Netherlands).

### 2.2 Methods

#### 2.2.1 Electrospinning conditions

The electrospun nanofiber mat selected as the reference system was processed using a 7% PVA aqueous solution at the following conditions: 12 kV as the voltage applied; 0.4 mL/h as the flow rate; 10 cm as the distance between the tip of the needle and the collector. In addition, Sodium Carbonate (SC) or Citric Acid (CA) was added to the raw PVA solution used for the electrospinning process at concentrations of 2 and 3 wt.%, respectively, in order to obtain SC or CA loaded mats. A combined mat formed from two independent syringes by alternative SC-loaded and CA-loaded layers was also evaluated. The effect of the presence of the compounds was analysed by determining the modifications produced on the water vapour absorption capacity.

#### 2.2.2 Physicochemical characterization of PVA solutions

The pH of the aqueous PVA solutions was determined by using a CyberScan pH 1500 (Eutech Instruments), whereas the electrical conductivity was measured with a EC-Meter Basic 30+ (Crison instruments) equipment. The density was obtained by means of a Densito 30PX Portable Density Meter (Mettler Toledo). All the measurements were determined at 25°C.

Viscosity measurements of PVA solution were carried out by means of an AR2000 (TA Instruments, New Castle, DE, USA) rheometer. All the rheological measurements were carried out at 25°C using 60 mm diameter aluminium serrated plates. Flow curves from 0.1 to 10 Pa were carried out in order to obtain the shear viscosity.

#### 2.2.3 Mechanical characterization of mats

Oscillatory dynamic tensile tests were carried out with a RSA3 (TA Instruments, New Castle, DE, USA), using rectangular specimens. Firstly, strain sweep tests were performed to define the linear viscoelastic region. Subsequently, frequency sweep tests were carried out from 0.01 to 20 Hz, at constant strain amplitude (between 0.01 and 0.30%, within the linear viscoelastic region).

Uniaxial tensile tests were performed at constant extensional rate of 1 mm/min up to breakup by using the RSA3 equipment. Tensile strength parameters were evaluated from at least three duplicates for each product obtained at 25°C.

### 2.2.4 Scanning Electron Microscopy (SEM)

Images of the fibres were obtained using a JEOL 6460LV (Tokyo, Japan) at an acceleration voltage of 10 kV, where the distance between the sample and the detector was between 2 and 5 mm. The specimens were previously coated with a gold film. Image analysis, using ImageJ software, was used to obtain the diameter of the fibres from each SEM image.

### 2.2.5 Water vapour absorption

The vapour absorption of electrospun mats was measured in controlled atmospheres. Thus, samples were previously dried in an oven at 50°C for 24h and then left until equilibrium at four different relative humidity: 32.8, 52.9, 75.3 and 100% HR. Samples were weighted before and after being kept into the controlled atmospheres, the water uptake was calculated as follows:

$$\% \text{ Water Uptake} = \frac{W_f - W_d}{W_d} \times 100$$

Where  $W_f$  is the weight of the sample after reaching the equilibrium into the controlled atmosphere and  $W_d$  is the weight of the dried sample.

## III. RESULTS AND DISCUSSION

### 3.1 PVA aqueous solutions

Figure 1 shows values of conductivity, density and dynamic viscosity for the PVA aqueous solution studied. The pH value found for the PVA aqueous solutions is slightly acid ( $5.3 \pm 0.1$ ), being similar to that one found for distilled water, which has been associated to presence of solved  $\text{CO}_2$  (Company & Kemmer, 1979). As may be observed, the presence of PVA increases the conductivity of water. However, this increase, which fits to a second degree polynomial equation, is not as high as the one found for inorganic salts, which typically fits to an exponential equation.

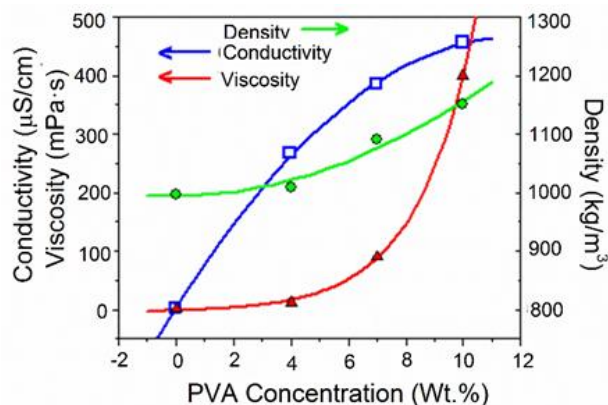


**FIGURE 1. ELECTRICAL CONDUCTIVITY, DENSITY AND DYNAMIC VISCOSITY FOR PVA DISSOLVED IN WATER AT FOUR DIFFERENT CONCENTRATIONS (0, 4, 7 AND 10 WT.%) AT 25°C**

The increase in PVA concentration also involves an increase in density, fitting a slow increasing second degree polynomial equation. As for the viscosity, PVA aqueous solutions show a Newtonian behaviour within the concentration range studied (from 0 to 10 wt.% PVA). Zadeh et al.(2014) found similar results but they obtained small deviations for PVA concentrations above 7 wt.%. As may be observed in Figure 1, the change in PVA concentration has a marked influence on the apparent viscosity, which fits to an exponential equation. In view of these results it is expected that the electrospinning process will show a strong dependence on the concentration of the PVA aqueous solutions.

### 3.2 PVA-based electrospun nanofiber mats

#### 3.2.1 Scanning Electron Microscopy

Figure 2 shows the SEM images of electrospinning mats obtained at the selected conditions (12kV, 0.4 mL/min and 10 cm distance) as a function of PVA content. As may be observed in this figure, the fibres obtained from each solution are randomly distributed on the collected final mat, forming a non-woven network. The fibres obtained show diameters

corresponding to the nanoscale, whose thickness depends on the processing time. The fibres obtained from the 7 wt.% PVA solution show a mean diameter of  $172 \pm 6$  nm, which corresponds to a specific surface in the order of  $10^7 \text{ m}^{-1}$ . This means that an electrospun nanofiber mat having a volume of  $1 \text{ cm}^3$ , would possess an exposed surface of ca.  $17 \text{ m}^2$ .

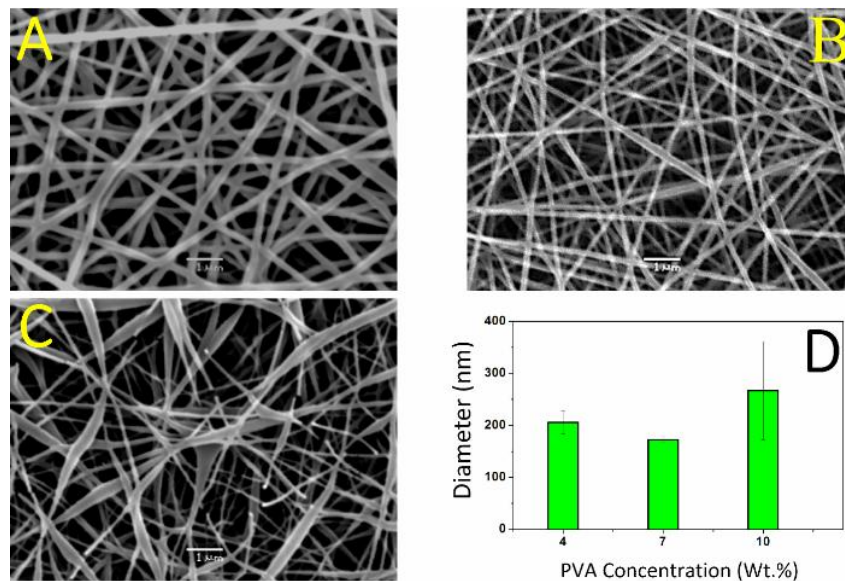


**FIGURE 2. SEM MICROSCOPY IMAGES OF A MAT MADE FROM 4 (A), 7 (B) AND 10 (C) WT. % PVA SOLUTIONS, 12 kV AND 0.4 mL/h, AS WELL AS BAR GRAPH SUMMARIZING THE MEAN NANOFIBER DIAMETER.**

As may be seen in this figure, more specifically in Fig. 2D, an increase in PVA content from 4 to 7 wt.% leads to an apparent reduction in the average diameter. A further increase also tends to produce thinner fibres but in this case they are combined with higher sizes, such that a much wider distribution may be clearly observed. Therefore, an intermediate value (i.e. 7 wt.% PVA) seems to be the most convenient concentration to obtain small and fairly uniform nanofiber diameters.

Figure 3 shows SEM images of electrospun nanofiber mats obtained from a 7 wt.% PVA solution at 0.4 mL/h flow rate, 10 cm distance and different voltage values. An increase in electric potential difference from 9 to 12 kV leads to a network enhancement in the nanofiber mat obtained since a clear reduction in average diameter takes place. A further reduction can be obtained by increasing the voltage up to 15 kV, however only a 20% reduction in diameter is involved in this later enhancement. It is also apparent that the lowest voltage value also gives rise to a wide distribution of sizes.

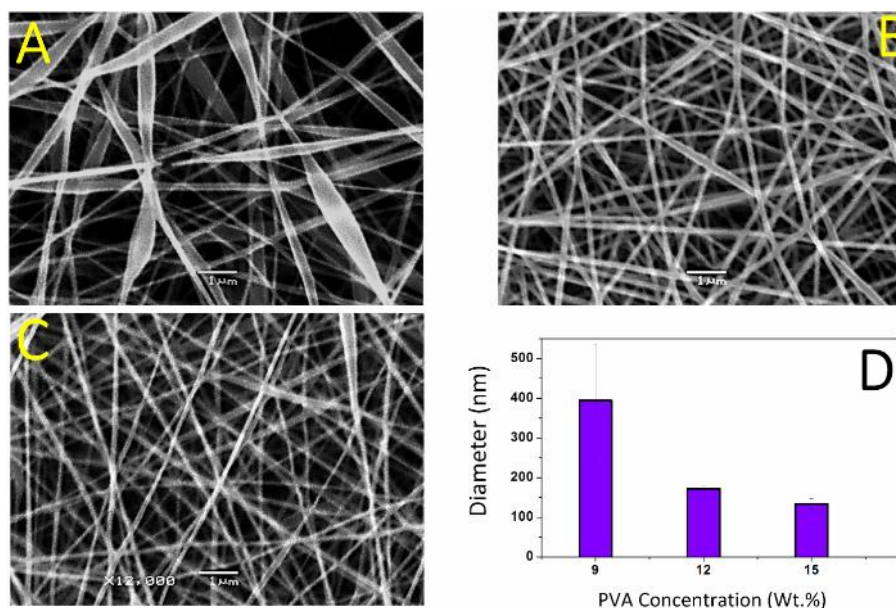


**FIGURE 3. SEM MICROSCOPY IMAGES OF A MAT MADE FROM 9 (A), 12 (B) AND 15 (C) kV, 7 wt.% PVA and 0.4 mL/h, AS WELL AS BAR GRAPH SUMMARIZING THE MEAN NANOFIBER DIAMETER.**

### 3.2.2 Rheological characterization

Dynamic frequency sweep tests were carried out in tension mode to obtain the mechanical spectrum of the nano fiber mat prepared at the reference conditions (7 wt.% PVA, 12kV, 0.4 mL/min and 10 cm). This measurement involves the application of constant uniaxial stress amplitude (within the linear viscoelastic range) at frequencies ranging from 0.01 to 20 Hz. The mechanical spectrum obtained, which is plotted in Fig. 4, reflects a typical behaviour of a solid viscoelastic film, where the elastic response ( $E'$ ) is much higher than the viscous response ( $E''$ ). Moreover, both moduli (particularly  $E'$ ) show a fairly small dependence on frequency. The value of  $E'$  (in the order of  $10^8$ Pa) also reflects the suitable mechanical properties of the mat. In addition, the loss tangent (ranging from 0.2 to 0.06) indicates the clear predominance of the elastic component of the viscoelastic response.

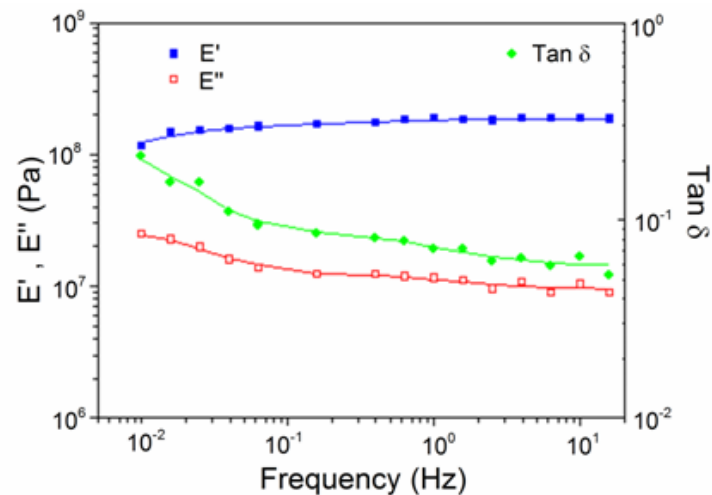


**FIGURE 4. LINEAR VISCOELASTIC PROPERTIES AS A FUNCTION OF THE FREQUENCY OF MAT MADE FROM 7 wt. % PVA AQUEOUS SOLUTION, 12 kV and 0.4 mL/h**

### 3.2.3 Tensile tests

The second test carried out in order to accomplish the mechanical characterization of the nanofiber mat was a uniaxial tensile test up to breakup, which gives rise to the stress-strain curve. This test consists in the application of an elongational uniaxial stress, which is monitored at constant rate over time. Figure 5 shows the stress-strain curve for the reference PVA mat.

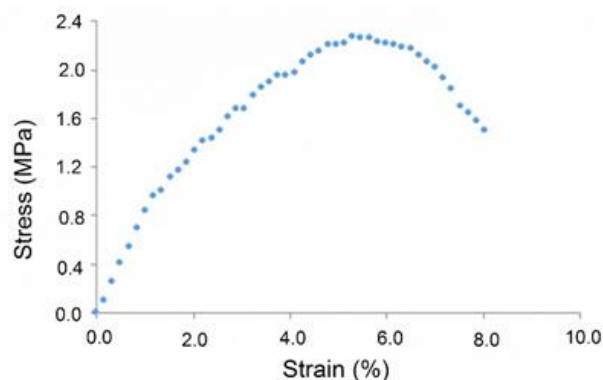


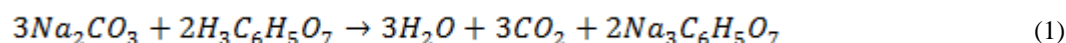
**FIGURE 5. STRESS-STRAIN CURVE FOR MATS AT 7 wt.% AQUEOUS SOLUTION PVA, 12 kV and 0.4 mL/h.**

A linear region of large slope, which is related to a good resistance against small strains and defines the Young's modulus ( $E$ ), characterizes the beginning of the stress-strain curve. This region is followed by a continuous increase in stress, taking place with progressively lower slope, up to a maximum value reached at the plastic deformation region. After this maximum value, the stress goes down as a consequence of the reduction of the area of the probe. Finally, the fracture of the specimen takes place. As may be observed, the strain at break is lower than 10%. The  $E$  obtained for the mat of nanofibers is around  $8.0 \cdot 10^7$  Pa. This result is slightly higher than those obtained by other authors using different electrospinning techniques:  $4.13 \cdot 10^7$  Pa (Chen et al., 2011);  $4.95 \cdot 10^7$  Pa (Li, Suo, & Deng, 2010) and  $6.85 \cdot 10^7$  Pa (Strawhecker & Manias, 2000).

Finally, the value of the maximum stress found is around  $2.4 \cdot 10^6$  Pa. In any case, these results are in the order of magnitude of the typical values obtained for commercial polymer materials such as those reported by Greesh & Luyt (2015) for Polystyrene-based materials.

### 3.2.4 Electrospun nanofiber mats loaded with inorganic compounds

One of the advantages of using this kind of materials is their ability to incorporate a wide variety of soluble compounds, which may confer interesting properties in some relevant applications such as in active packaging. One of these properties is the ability to absorb water from the environment. Thus, the effect of adding a soluble compound to 7 wt.% PVA aqueous solution on the electrospun mat was evaluated. This compound was either Sodium Carbonate (SC) or Citric Acid (CA). It should be noticed that both compounds cannot be simultaneously added since they spontaneously react to produce the following reaction that requires the presence of water to be initiated:



Therefore it is worth mentioning that SC and CA may coexist in solid state without reacting provided that the moisture content is low enough. As a consequence of this, a combined PVA-based electrospun nanofiber mat formed by alternative SC-loaded and CA-loaded layers may be also obtained. The effect of the presence of these compounds (SC and/or CA) was analysed by determining the modifications produced on the water vapour absorption capacity.

### 3.2.5 Moisture absorption

Figure 6 shows results obtained from moisture absorption by using Eq. (1) after keeping samples over 15 days in a controlled atmosphere at 32.8%, 52.9%, 75.3% and 100% RH. As may be observed, all mats exhibit a high water absorption capacity, which increases according to the RH.

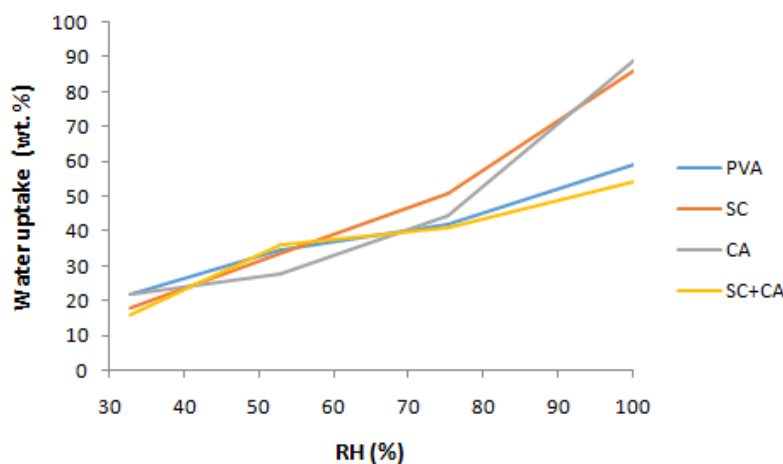


FIGURE 6. PERCENTAGE OF WATER ABSORPTION OF MATS AS A FUNCTION OF RH (%)

This figure shows that all the mats have almost the same water absorption capacity up to a certain value of RH. However after this value (c.a. 75% RH) PVA mats loaded only with SC or CA show higher water absorption ability than the others. These results reflect the higher hydrophilic character of both compounds. However, a striking result seems to be obtained for the moisture absorption of mixed SC+CA mat, since it turns to be much lower than the values obtained for single loaded SC or CA mats, showing similar value to that of the unloaded PVA mat. This behaviour can be related to the occurrence of the above-mentioned chemical reaction, taking place between the SC and the CA when critical moisture content is exceeded. In fact, the expected increase in weight due to moisture absorption associated to the hydrophilic character of SC and CA seems to be counterbalanced by some weight loss (e.g. due to  $\text{CO}_2$  release).

### 3.2.6 Scanning Electron Microscopy (SEM)

Figure 7 shows SEM images of mats containing SC and CA where formation of nanofibers can be observed. The PVA concentration was 7 wt.%, while the SC/PVA and CA/PVA was 20/80 and 30/70, respectively. Note that these proportions are in accordance with the stoichiometry between the SC and the CA of the above-described chemical equation.



Initially, the ratio SC/PVA 30/70 was also studied, however mats changed from 2D to 3D structure (cotton-like structure), which showed a fairly poor uniformity, as a consequence of the electrostatic repulsions. According to Bhardwaj y Kundu (2010) solutions which contains a high concentration of charges are extremely unstable when an electrostatic field is applied. This effect is related to fast and random movements of the strand, which induces the 3D structure, as well as a decrease in fibres uniformity.

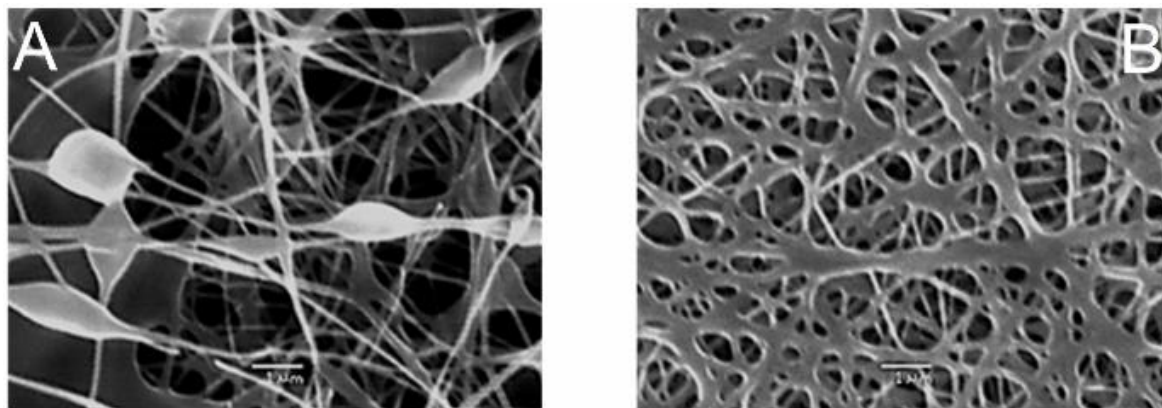


**FIGURE 7. SEM IMAGES OF NANOFIBERS OBTAINED AFTER ADDING EITHER SC (A) OR CA (B) TO AQUEOUS SOLUTIONS OF 7 wt.% PVA.**

As may be deduced from SEM images both mats show a very different morphology with regard to the reference system and to each other. Thus, the mat containing SC is characterized by an alternation of fibres with a reduced diameter (~150 nm) and fibres with beads that cannot observe that in the reference system. This effect is related with the strong presence of charges in the solution.

On the other hand, the presence of CA induces formation of fairly planar fibres with thicker diameter values (~350 nm). The fibres also seem to have a higher number of “melted” points, suggesting a poorer efficiency of solvent elimination. Zhang et al. (2005) also found this effect in PVA solutions with a low degree of hydrolysis. They related this morphology to mats which retain solvent when the fiber is placed on the collector.

#### IV. CONCLUSION

Electrospinning of PVA solutions at moderate concentrations leads to mats that consist of a network of randomly distributed non-woven fibres showing uniform sizes, in the order of 200 nm. Viscoelastic characterization from rheological measurements shows the typical response for a solid viscoelastic film. Moreover, parameters from stress-strain curves indicate that the mats obtained from the electrospun process are suitable for a commercial use.

In addition, it has been shown that water-soluble compounds may be incorporated into electrospun nanofiber mats, although they may induce marked changes in their morphological characteristics. Thus, addition of Sodium Carbonate involves occurrence of beads, due to the increase in electrostatic charges, whereas Sodium Citrate induce an increase in fiber size, related to a loss of solvent evaporation efficiency.

SC/PVA and CA/PVA electrospun nanofiber mats show higher vapour sorption capacity than those processed only with PVA, provided that the relative humidity exceeds a critical value. Interestingly, however, mats containing SC, CA and PVA show similar vapour sorption behaviour. This effect suggests that a chemical reaction between Sodium Carbonate and Citric Acid to release carbon dioxide takes place above 70% RH.

After these results, it may be concluded that electrospinning shows an apparent potential interest for its application as carbon dioxide emitter systems in active food packaging.

#### ACKNOWLEDGEMENTS

This work is part of a research project sponsored “Ministerio de Economía y Competitividad” from Spanish Government (Ref. CTQ2015-71164-P). The authors gratefully acknowledge their financial support. The authors also acknowledge to the Microscopy service (CITIUS-Universidad de Sevilla) for providing full access and assistance to the JEOL 6460LV equipment.

## REFERENCES

- [1] Arvanitoyannis, I., & Oikonomou, G. (2012). Active and Intelligent Packaging. In *Modified Atmosphere and Active Packaging Technologies* (pp. 627–662). CRC Press. <http://doi.org/doi:10.1201/b12174-21>
- [2] Bhardwaj, N., & Kundu, S. C. (2010). Electrospinning: A fascinating fiber fabrication technique. *Biotechnology Advances*, 28(3), 325–347. <http://doi.org/10.1016/j.biotechadv.2010.01.004>
- [3] Bhushani, J. A., & Anandharamakrishnan, C. (2014). Electrospinning and electrospraying techniques: Potential food based applications. *Trends in Food Science & Technology*, 38(1), 21–33. <http://doi.org/http://dx.doi.org/10.1016/j.tifs.2014.03.004>
- [4] Bodbodak, S., & Rafiee, Z. (2016). 3 - Recent trends in active packaging in fruits and vegetables. In M. W. Siddiqui (Ed.), *Eco-Friendly Technology for Postharvest Produce Quality* (pp. 77–125). Academic Press. <http://doi.org/http://dx.doi.org/10.1016/B978-0-12-804313-4.00003-7>
- [5] Chen, C., Torrents, A., Kulinsky, L., Nelson, R. D., Madou, M. J., Valdevit, L., & LaRue, J. C. (2011). Mechanical characterizations of cast Poly(3,4-ethylenedioxythiophene):Poly(styrenesulfonate)/Polyvinyl Alcohol thin films. *Synthetic Metals*, 161(21-22), 2259–2267. <http://doi.org/10.1016/j.synthmet.2011.08.031>
- [6] Company, N. C., & Kemmer, F. N. (1979). *The NALCO water handbook*. McGraw-Hill.
- [7] Fernandez, A., Torres-Giner, S., & Lagaron, J. M. (2009). Novel route to stabilization of bioactive antioxidants by encapsulation in electrospun fibers of zein prolamine. *Food Hydrocolloids*, 23(5), 1427–1432. <http://doi.org/10.1016/j.foodhyd.2008.10.011>
- [8] Greesh, N., & Luyt, A. S. (2015). Preparation of Multiphase Poly(Styrene-co-Butyl acrylate)/Wax-Clay Nanocomposites via Miniemulsion Polymerization. *International Journal of Engineering Research & Science*, 1(6), 38–49.
- [9] Janjarasskul, T., Tananuwong, K., Kongpensook, V., Tantratian, S., & Kokpol, S. (2016). Shelf life extension of sponge cake by active packaging as an alternative to direct addition of chemical preservatives. *{LWT} - Food Science and Technology*, 72, 166–174. <http://doi.org/http://dx.doi.org/10.1016/j.lwt.2016.04.049>
- [10] Li, J., Suo, J., & Deng, R. (2010). Structure, mechanical, and swelling behaviors of poly (vinyl alcohol)/SiO<sub>2</sub> hybrid membranes. *Journal of Reinforced Plastics and Composites*, 29(4), 618–629.
- [11] Lucera, A., Conte, A., & Nobile, M. A. Del. (2016). Chapter 25 - Volatile Compounds Usage in Active Packaging Systems. In J. Barros-Velázquez (Ed.), *Antimicrobial Food Packaging* (pp. 319–327). San Diego: Academic Press. <http://doi.org/http://dx.doi.org/10.1016/B978-0-12-800723-5.00025-5>
- [12] Sandhya. (2010). Modified atmosphere packaging of fresh produce: Current status and future needs. *{LWT} - Food Science and Technology*, 43(3), 381–392. <http://doi.org/http://dx.doi.org/10.1016/j.lwt.2009.05.018>
- [13] Siripatrawan, U., & Vitchayakitti, W. (2016). Improving functional properties of chitosan films as active food packaging by incorporating with propolis. *Food Hydrocolloids*, 61, 695–702. <http://doi.org/http://dx.doi.org/10.1016/j.foodhyd.2016.06.001>
- [14] Strawhecker, K. E., & Manias, E. (2000). Structure and properties of poly(vinyl alcohol)/Na<sup>+</sup> montmorillonite nanocomposites. *Chemistry of Materials*, 12(10), 2943–2949. <http://doi.org/10.1021/cm000506g>
- [15] Tang, X., Liu, Y., Hou, H., & You, T. (2011). A nonenzymatic sensor for xanthine based on electrospun carbon nanofibers modified electrode. *Talanta*, 83(5), 1410–1414. <http://doi.org/10.1016/j.talanta.2010.11.019>
- [16] Zadeh, M. M. A., Keyanpour-Rad, M., & Ebadzadeh, T. (2014). Effect of viscosity of polyvinyl alcohol solution on morphology of the electrospun mullite nanofibres. *Ceramics International*, 40(4), 5461–5466. <http://doi.org/http://dx.doi.org/10.1016/j.ceramint.2013.10.132>
- [17] Zhang, C. X., Yuan, X. Y., Wu, L. L., Han, Y., & Sheng, J. (2005). Study on morphology of electrospun poly(vinyl alcohol) mats. *European Polymer Journal*, 41(3), 423–432. <http://doi.org/10.1016/j.europolymj.2004.10.027>